

# NJC

Accepted Manuscript



This is an *Accepted Manuscript*, which has been through the Royal Society of Chemistry peer review process and has been accepted for publication.

*Accepted Manuscripts* are published online shortly after acceptance, before technical editing, formatting and proof reading. Using this free service, authors can make their results available to the community, in citable form, before we publish the edited article. We will replace this *Accepted Manuscript* with the edited and formatted *Advance Article* as soon as it is available.

You can find more information about *Accepted Manuscripts* in the [Information for Authors](#).

Please note that technical editing may introduce minor changes to the text and/or graphics, which may alter content. The journal's standard [Terms & Conditions](#) and the [Ethical guidelines](#) still apply. In no event shall the Royal Society of Chemistry be held responsible for any errors or omissions in this *Accepted Manuscript* or any consequences arising from the use of any information it contains.

## ARTICLE

## Structure–property relationship study of bent-core mesogens with pyridine as central unit<sup>†</sup>

Cite this: DOI: 10.1039/x0xx00000x

J.M. Marković,<sup>a</sup> N.P. Trišović,<sup>\*a</sup> T. Tóth-Katona,<sup>b</sup> M.K. Milčić,<sup>c</sup> A.D. Marinković,<sup>a</sup> C. Zhang,<sup>d</sup> A.J. Jakli<sup>b,d</sup> and K. Fodor-Csorba<sup>b</sup>

Received 00th January 2012,

Accepted 00th January 2012

DOI: 10.1039/x0xx00000x

www.rsc.org/

Three series of bent-core mesogens having pyridine as central unit have been synthesized and characterized. A series of 2,6-diaminopyridine derivatives capable to form inter- and intramolecular hydrogen bonds exhibits very high melting points. A decrease in the polarity of the central part of the bent-core achieved by replacing the amide with ester linkages results in derivatives with lower melting points and formation of B2- and B7-like mesophases. The introduction of the olefinic groups, which connect the pyridine ring with the inner aromatic rings, helps to further lower the polarity of the central part in the five ring system and led to the formation of B1 and B7 phases. The phases have been determined by optical microscopy observations, differential scanning calorimetry (DSC) and confirmed by X-ray studies. The bending angles and polarity of the investigated five-ring systems have been calculated by density functional theory (DFT) method.

### Introduction

Pyridine presents an attractive structural unit to be incorporated in organic materials, due to its aromaticity, strong electron-withdrawing character, high dipolar interaction and pH sensitivity. It can be used in materials for second harmonic generation, optical parametric oscillation and electro-optic modulation.<sup>1–3</sup> The electron deficiency and therefore, the electron affinity of the pyridine ring results in a higher resistance to oxidation and better electron transport properties, than most aromatic systems.<sup>4</sup>

In search for materials with a new chemical architecture, bent-core mesogens have attracted significant attention in recent years. Their unusual properties result from a polar smectic order, and the appearance of different types of structural chirality, although the constituent molecules may be achiral.<sup>5</sup> Additionally, it has been demonstrated that this chirality can be switched in external electric fields.<sup>6</sup> In spite of the very large activity in making a large variety of bent-core molecules, mostly with 1,3-disubstituted benzene as central unit, only a limited number of mesogens containing pyridine as central unit have been reported so far.<sup>7–9</sup> Pyridine derivatives have also been used in mixtures with carboxylic acids to afford

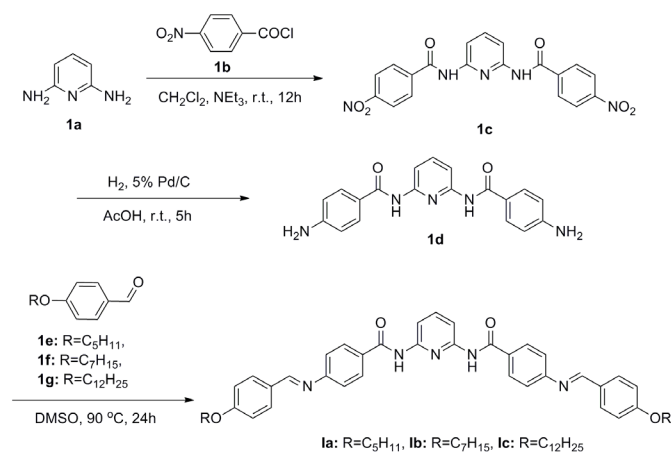
hydrogen-bonded bent-shaped complexes which arrange in different mesophases.<sup>10,11</sup>

In the present work we describe the synthesis and characterization of three series of symmetrical bent-core compounds with 2,6-disubstituted pyridine as central unit. These materials combine different linkages (amide (–CONH–), ester (–COO–), azomethine (–CH=NH–) and olefinic (–CH=CH–) with different chain lengths in the terminal chains. Because the compounds have a significant  $\pi$ -conjugation level, they are expected to have advanced electro-optical properties and potential application as organic electronic materials. The mesophases and transition temperatures of the investigated compounds have been further compared with the corresponding ones containing 1,3-disubstituted benzene as central unit which are available in the literature.

### Results and discussion

#### Materials synthesis

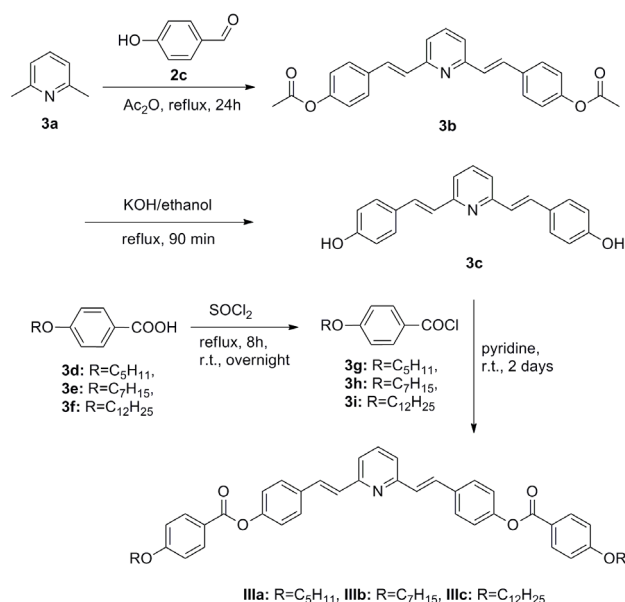
Compounds **1a–1c** were obtained by following the synthetic protocol presented in Scheme 1. 2,6-Diaminopyridine (**1a**) reacted with 4-nitrobenzoyl chloride (**1b**) in pyridine to form *N,N'*-bis(4-nitrobenzoyl)-2,6-diaminopyridine (**1c**) according to

Scheme 1 Synthetic route for compounds **Ia–Ic**

the procedure described by Gamliel *et al.*<sup>12</sup> The nitro group was reduced to *N,N'*-bis(4-aminobenzoyl)-2,6-diaminopyridine (**1d**) by palladium-catalyzed hydrogenation. Finally, *N,N'*-bis[4-(4-*n*-alkoxyphenyl)methyliminobenzoyl]-2,6-diaminopyridines (**1a–1c**) were obtained from the condensation reaction between **1d** and the corresponding 4-*n*-alkoxybenzaldehydes (**1e–1g**) in DMSO. 4-*n*-Alkoxybenzaldehydes (**1e–1g**) were obtained by the already known methodology.<sup>13</sup>

The synthesis of di[4-(4-*n*-alkoxyphenylmethyliminomethyl)phenyl]pyridine-2,6-dicarboxylates (**IIa–IIc**) is accomplished in three steps (Scheme 2). 2,6-Dipicolinic acid (**2a**) was converted into the corresponding chloride (**2b**) which further reacted with 4-hydroxybenzaldehyde (**2c**) to form the ester of dipicolinic acid (**2d**). Similarly to series **I**, compounds **IIa–IIc** were prepared by the condensation reaction between compound **2d** and the corresponding 4-*n*-alkoxyanilines (**2e–2g**). 4-*n*-Alkoxyanilines (**2e–2g**) were synthesized according to procedures described in the literature.<sup>14</sup>

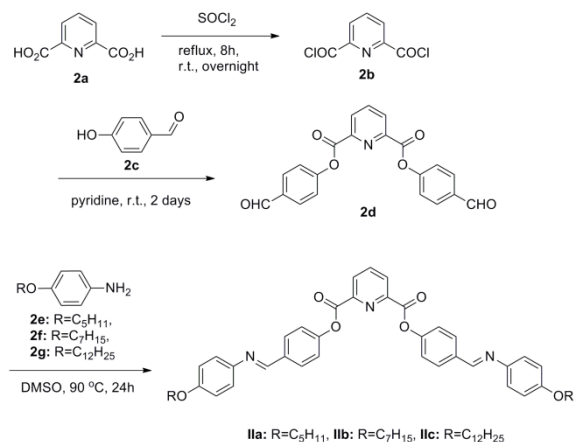
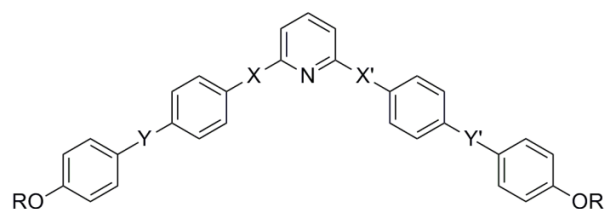
The synthesis of 2,6-bis[2-(4-(4-alkoxybenzoyloxy)phenyl)ethenyl]pyridines (**IIIa–IIIc**) is presented in Scheme 3. 2,6-Bis[2-(4-hydroxyphenyl)ethenyl]pyridine (**3c**) was prepared according to the procedure described by Bergmann and Pinchas.<sup>15</sup> Condensation of 2,6-lutidine (**3a**) with excess 4-hydroxybenzaldehyde (**2c**) in acetic anhydride at the reflux

Scheme 3 Synthetic route for compounds **IIIa–IIIc**

temperature afforded 2,6-bis[2-(4-ethanoyloxyphenyl)ethenyl]pyridine (**3b**), base catalysed hydrolysis of which led to **3c**. In the final step, compounds **IIIa–IIIc** were obtained by acylation of **3c** with the corresponding 4-*n*-alkoxybenzoyl chlorides (**3g–3i**). Acid chlorides were firstly prepared by using the reaction between the corresponding 4-*n*-alkoxybenzoic acids (**3d–3f**) with thionyl chloride according to the known procedure.<sup>16</sup>

### Mesomorphic properties

The chemical structures of the new bent-core molecules are summarized in Figure 1. Because the mesogens reported up to now contain in most cases a Schiff's base unit as linkage,<sup>17</sup> azomethine-based compounds have been firstly synthesized in this study. It has already been demonstrated that the

Scheme 2 Synthetic route for compounds **IIa–IIc**

Compound	X	X'	Y	Y'	R
<b>Ia</b>	CONH	NHCO	CH=N	N=CH	C <sub>6</sub> H <sub>11</sub>
<b>Ib</b>	CONH	NHCO	CH=N	N=CH	C <sub>7</sub> H <sub>15</sub>
<b>Ic</b>	CONH	NHCO	CH=N	N=CH	C <sub>12</sub> H <sub>25</sub>
<b>IIa</b>	OOC	COO	N=CH	CH=N	C <sub>6</sub> H <sub>11</sub>
<b>IIb</b>	OOC	COO	N=CH	CH=N	C <sub>7</sub> H <sub>15</sub>
<b>IIc</b>	OOC	COO	N=CH	CH=N	C <sub>12</sub> H <sub>25</sub>
<b>IIIa</b>	CH=CH	CH=CH	COO	OOC	C <sub>6</sub> H <sub>11</sub>
<b>IIIb</b>	CH=CH	CH=CH	COO	OOC	C <sub>7</sub> H <sub>15</sub>
<b>IIIc</b>	CH=CH	CH=CH	COO	OOC	C <sub>12</sub> H <sub>25</sub>

Figure 1 Chemical structures of the investigated bent-shaped compounds

introduction of the amide group has a positive effect on mesophase stabilisation of bent-core mesogens with a small increase of clearing temperatures.<sup>18,19</sup> In this case the combination of the amide and azomethine groups has resulted in solids **Ia–Ic** with extremely high clearing temperatures (>300°C). This is due to the polarization, induced by the electron-withdrawing pyridine ring, and the intramolecular hydrogen bonding. In comparison with similar compounds **IIa–IIc**, but with ester linkages, we see that the less polar ester linkage results in a decrease of the clearing points by about 50°C. Generally, the amide group confers structural rigidity due to its partial double bond character, which results in higher clearing points of mesogens. The transition temperatures and enthalpies of series **II** and **III**, obtained from DSC at a scan rate of 5 K min<sup>-1</sup> in the second heating and cooling scans, are presented in Table 1. The DSC curves for series **III** are presented in Electronic Supplementary Information (Figure S1). Due to the high temperature ranges, the azomethine compounds **IIa–IIc** partially decomposed before melting. This decomposition inhibits the mesophase formation in the second heating and cooling scans of the DSC experiments. In comparison with analogous systems possessing 1,3-disubstituted benzene as central unit<sup>20</sup>, pyridine increases the clearing point by almost 100°C. Compound **IIa**, with the shortest terminal chain, is a crystalline solid without mesomorphic properties, while compound **IIb** is more stable, and its mesophase transition is clearly visible by POM during cooling (Figure 2a), although this transition is not observed by DSC.

Compound **IIc**, with the longest terminal chain and the lowest clearing point, exhibits mesomorphic properties, which are observed both by DSC and POM (Figure 2b). The most stable compounds with the lowest clearing temperatures (**IIIa–IIIc**) have been obtained by combining the ester linkage with the olefinic group, the least polar linkage used in this study. As also expected, the clearing temperatures of compounds of series **III** decrease with growing terminal chain length (Table 1). Compound **IIIa** with the shortest terminal chain length does not exhibit mesophase properties, while **IIIb** and **IIIc** do.

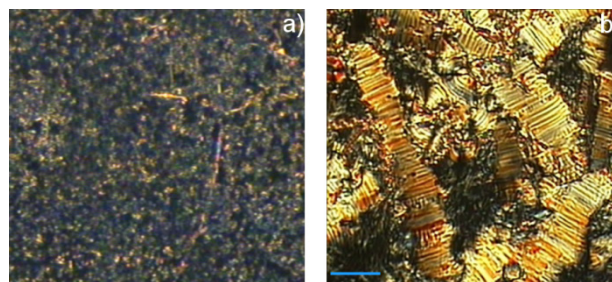


**Figure 2** Optical photomicrographs (crossed polarizers) of compound a) **IIb** - T=257°C: formation of B7-like phase; b) **IIc** - T=241°C: formation of stripes resembling to the B2 phase

The identification of the mesophases has been aided by using Polarizing Optical Microscopy (POM). Compound **IIb** shows a monotropic mesophase, although no enthalpy change related to this transition was observed by DSC. On cooling from the isotropic phase, the growth of spiral birefringent domains, resembling to the B7 phase, is seen in a less than 1°C before it crystallized (see Figure 2a). Compound **IIc** shows an enantiotropic mesophase behaviour which is characterised by: i) the formation of two mesophases during heating, the transition between which is observed by the colour change (ESI Figure S2), ii) on cooling transition from isotropic to the first mesophase is presented by the formation of stripes resembling to the B2 phase (Figure 2b) also characterised by the narrow mesomorphic range.

On cooling from the isotropic liquid state, compound **IIIb** forms batonnets, which rapidly turn into branched lancets and finally coalesce into a structured mosaic-like texture with some spherulitic domains (Figure 3). This texture resembles to the columnar B1 phase. Compound **IIIc** forms helical filaments and circular domains of low and high birefringence on slow cooling from the isotropic phase. These spiral germs resemble to the B7 phase, Figure 4.

**Table 1** The transition temperatures and enthalpies seen by DSC in the second heating and cooling scans at 5 K min<sup>-1</sup> rate

Compound	Mode	Cr1	T(°C) [ $\Delta H(\text{J g}^{-1})$ ]	Cr2	T(°C) [ $\Delta H(\text{J g}^{-1})$ ]	Mesophase	T(°C) [ $\Delta H(\text{J g}^{-1})$ ]	I
<b>Ia</b> <sup>1</sup>	Heating	·	decomposition	-	-	-	>300	·
<b>Ib</b> <sup>1</sup>	Heating	·	decomposition	-	-	-	>300	·
<b>Ic</b> <sup>1</sup>	Heating	·	decomposition	-	-	-	>300	·
<b>IIa</b> <sup>1</sup>	Heating	·	253 [5.0]	·	275 [78.0]	-	-	·
	Cooling	·	268 [34.0]	-	-	-	-	·
<b>IIb</b> <sup>1</sup>	Heating	·	259 [65.3]	-	-	-	-	·
	Cooling	·	259 [75.0]	-	-	-	-	·
<b>IIc</b> <sup>2,3</sup>	Heating	·	231	-	-	B2-like	244	·
	Cooling	·	234	-	-	B2-like	243	·
<b>IIIa</b>	Heating	·	200 [61.4]	-	-	-	-	·
	Cooling	·	191 [67.6]	-	-	-	-	·
<b>IIIb</b>	Heating <sup>4</sup>	·	179 [ $\Delta H_1$ ]	-	-	B1	186 [ $\Delta H_2$ ]	·
	Cooling	·	171 [46.8]	-	-	B1	186 [26.2]	·
<b>IIIc</b>	Heating	·	112 [16.9]	·	150 [46.5]	B7	169 [33.2]	·
	Cooling	·	105 [18.0]	·	150 [47.7]	B7	169 [36.1]	·

<sup>1</sup>strong decomposition occurs;

<sup>2</sup>transition temperatures are given for the first run due to the partial decomposition of the compound;

<sup>3</sup>no enthalpy data;

<sup>4</sup> $\Delta H_1 + \Delta H_2 = 74.1 \text{ J g}^{-1}$



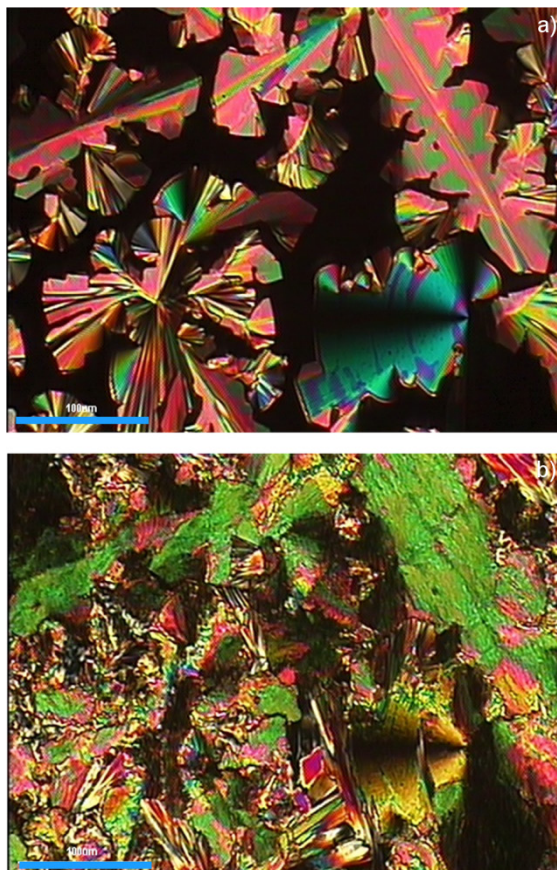


**Figure 3** Optical photomicrographs (crossed polarizers are parallel to picture edges) of a 5  $\mu\text{m}$  thick film with planar anchoring of compound **IIIb**: a)  $T=177.5^\circ\text{C}$ : formation of a columnar (B1) mesophase; b)  $T=163.8^\circ\text{C}$ : crystal phase

### X-ray studies

SAXS measurements were carried out on material **IIIc** that has a B7 phase between  $159^\circ\text{C}$  and  $140^\circ\text{C}$ . Summary of the results is shown in Figure 5. The 2-dimensional scattering pattern (Figure 5a) shows a main peak with a number of satellite peaks that correspond to a modulated smectic layers with periodicity of  $d=40.1\text{\AA}$ , which is basically independent of the temperature. The layer modulation also shows up in the small  $q$  range where the 2<sup>nd</sup> to 7<sup>th</sup> harmonics of the 30 nm modulation periodicity appears with decreasing intensity. The corresponding  $q$  dependence of the integrated intensities is shown in Figure 5b. The modulation periodicity  $b$  is almost linearly increasing on cooling from  $285\text{\AA}$  at  $158^\circ\text{C}$  to  $310\text{\AA}$  at  $146^\circ\text{C}$ , as shown in Figure 5c. The angle  $\gamma$  between the layer and modulation periodicities is slightly increasing from  $83.4^\circ$  at  $158^\circ\text{C}$  to  $84^\circ$  at  $146^\circ\text{C}$  (see Figure 5d). All these behaviours are typical for the layer modulated SmCPmod phases of bent-core molecules.<sup>21,22</sup> The main reason for the layer modulation is the polarization splay that leads to defects separating areas with different tilt directions that leads to regions with low packing efficiency. The need to improve the packing efficiently results in a



**Figure 4** Optical photomicrographs (crossed polarizers along the edges) of a  $5\mu\text{m}$  thick film with planar anchoring of compound **IIIc**: a)  $T=162^\circ\text{C}$ : formation of helical filaments and beaded filaments characteristic of a B7 phase; b)  $T=145^\circ\text{C}$ : crystal phasetext of the article should go here with headings as appropriate

decrease of the tilt angle, which would violate the constant layer spacing, forcing the layer modulation. For this reason, the larger is the tilt angle, the larger is the layer modulation amplitude, and the elastic energy penalty. To decrease this energy penalty, the modulation's period should increase. The observation of the increasing modulation periodicity therefore may be attributed to an increasing tilt angle toward lower temperatures. This is consistent with the model of Vaupotic *et al.*<sup>23</sup>, if the elastic term  $K_p(\theta)$  that stabilizes a finite splay of polarization increases with the tilt angle.

We attempted to do x-ray studies for **IIIb**, as well, but the transition temperatures were too high for the heat stage we have available in the synchrotron x-ray beam.

### Electro-optical measurements

Electro-optical and polarization current measurements were carried out, but no electro-optical switching and no polarization peaks were observed up to  $16\text{V}/\mu\text{m}$  for **IIIc** and  $8\text{V}/\mu\text{m}$  for **IIIb**, respectively. Those fields also mark the upper limit of fields we could apply without electric breakdown.

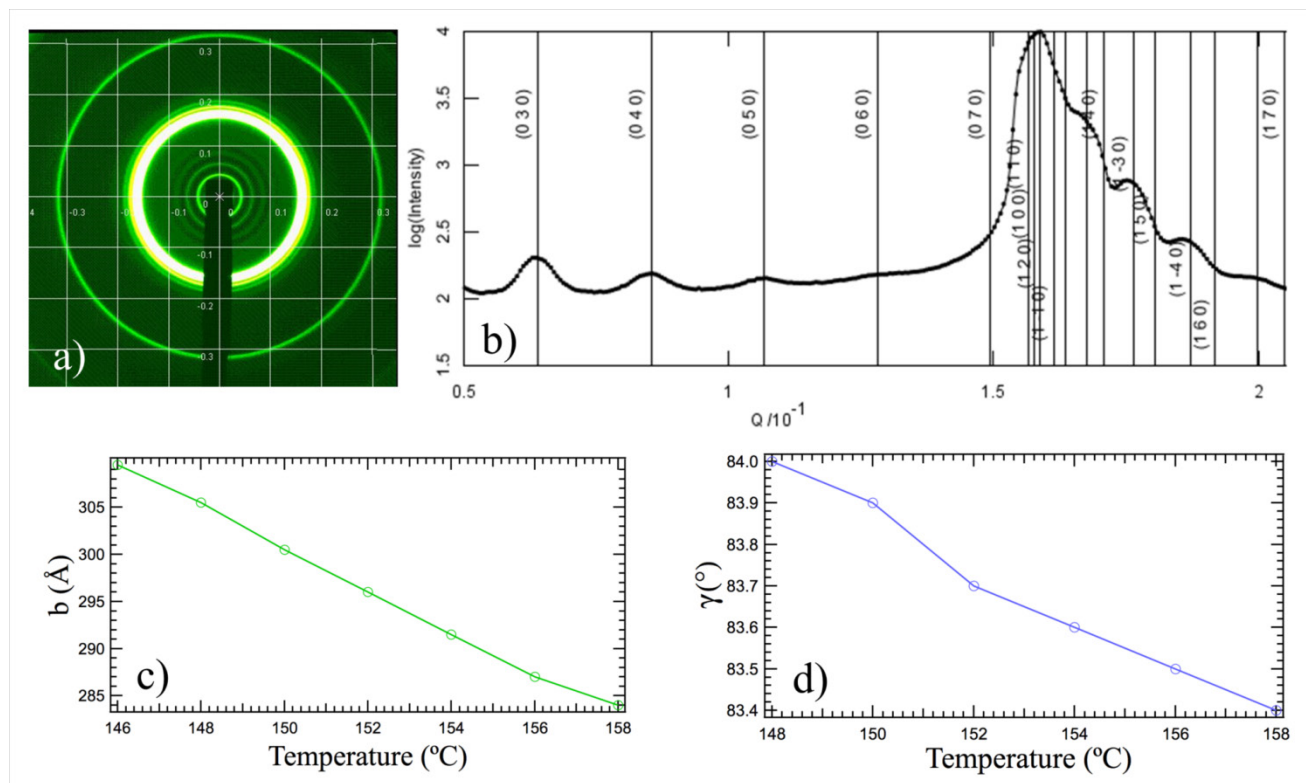


**Figure 5** Summary of the SAXS results on 3C in the B7 phase. (a) 2-D scattering pattern at 152 °C; (b) The corresponding  $q$  dependence of the scattered intensity; (c) The temperature dependence of the modulation period  $b$ ; (d) the temperature dependence of the angle between the layer periodicity ( $d=40.1\text{Å}$  in the entire B7 phase range) and the modulation period  $b$

Consequently we cannot tell whether the phases are ferroelectric or antiferroelectric. We note that the absence of electro-optical and polarization switching is quite usual in B7 and B1 materials.

### Quantum chemical calculations

Detailed density functional theory (DFT) calculations have been widely performed to shed light on the structure and polarity of bent-core mesogens.<sup>24-26</sup> Herein, the molecular properties of the investigated compounds have been elucidated by the DFT B3LYP/6-311G(d,p) method. To reduce the computational effort, all calculations have been performed on five-ring systems bearing the methoxy groups instead of the terminal chains (Figure 6). Their conformational behaviour is primarily determined by the rotation around the bond between the central pyridine ring and the neighbouring atoms, whereas the rotations in the wings are considered to have only a small influence.

The calculations have shown that there are three stable conformers for each of these systems. The stable conformers of the cores of systems **I**, **II** and **III** are shown in Figure 7. For the system **I**, the most stable conformer (**IA**) is symmetric (with the C2 rotation axis and plane of reflection; C2v point group), whereas, when the bond between the pyridine ring and the amide group is rotated for 180°, a less symmetric conformer

(**IB**) is obtained (with the C2 rotation axis, but without the plane of reflection, C2 point group). The structure of a less stable conformer (**IC**) can be regarded as a combination of **IA** and **IB**, and it is asymmetric. The relative energies, dipole moment components ( $\mu_x$ ,  $\mu_y$ ,  $\mu_z$ ), modulus ( $\mu$ ), and corresponding angles for these three conformers are presented in Table 2.

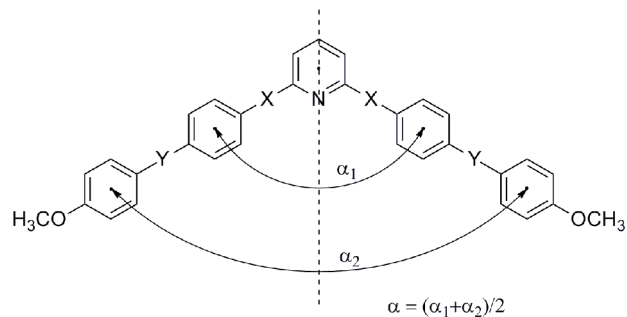


**Figure 6** Bent-core systems with bending angles,  $\alpha_1$  and  $\alpha_2$

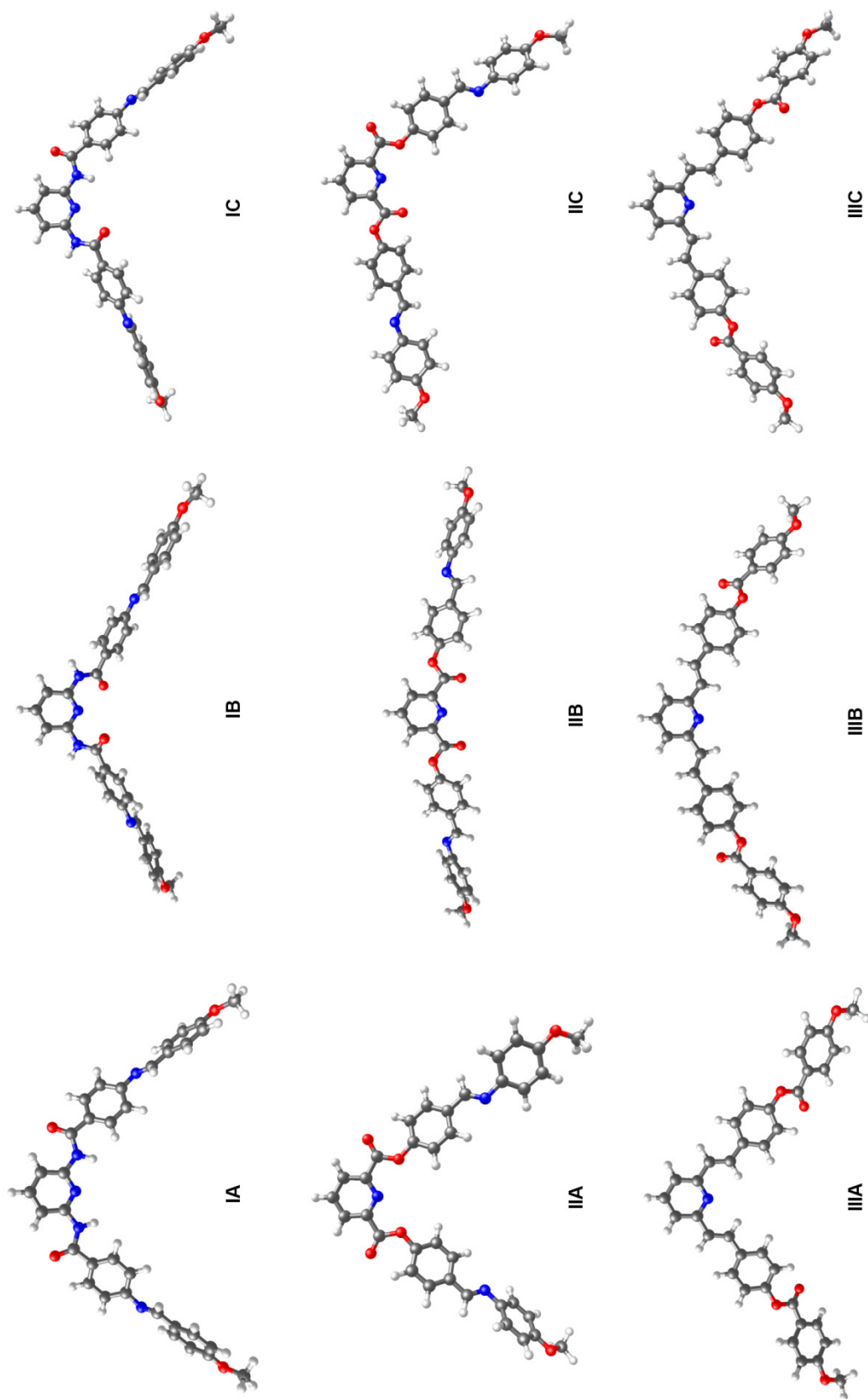


Figure 7 The stable conformers of the five-ring systems I, II and III

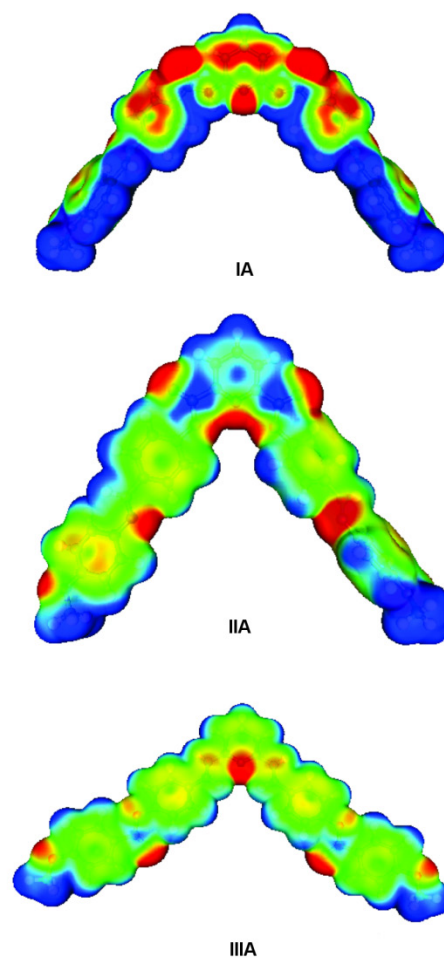


Table 2 shows that conformer **IA** is the most stable, due to formation of the intramolecular hydrogen bonds between the amide oxygen and hydrogen atoms from the pyridine ring. Those hydrogen bonds stabilise the structure by forming six-member rings. The dipole moments are largest for the most stable conformer (**IA**). Conformer **IB** is almost non-polar, caused by the molecular symmetry (Table 2). The relative energy and dipole moment values of conformer **IC** are between those of conformers **IA** and **IB**. This is expected due to its molecular structure (hydrogen bond is formed only in one part of the molecule).

The structural characteristics of the conformers of system **II** are similar to the corresponding conformers of system **I** (Figure 7). Their relative energies and dipole moments are presented in Table 2. **IIA**, having intramolecular hydrogen bonds between the oxygen and hydrogen atoms, is the most stable. As these hydrogen bonds are weaker, the energy differences between the conformers are smaller than of the conformers of the system **I**. It can also be seen that the energy and dipole moment values of **IIC** are between the conformers **IIA** and **IIB**.

System **III** has structural properties similar to the previous ones. The differences in energy between conformers **IIIA**, **IIIB** and **IIIC** are significantly smaller, because there is not any polar atom near the pyridine ring. This system is less polar, and the electrostatic potential surface is much more neutral (green colour represents non-polar part of molecule; Figure 8). The dipole moment values have the same trend as for the systems **I** and **II**, but with lower values (Table 2).

We have found that the obtained values of the bending angle are in a good agreement not only with previous calculations for similar systems at different levels of theory<sup>24-26</sup> but also with the bending angles obtained by single-crystal X-ray study of three-ring compounds which can be regarded as structural constituents of the investigated compounds. The highest/lowest bending angles  $\alpha$  are found for the system **I/II** (Table 2). Literature survey shows that *N,N'*-dibenzoyl-2,6-diaminopyridine<sup>27</sup> exhibits a bending angle of 123.5° which is in a good agreement with the value obtained for **IA** (Table 2).



**Figure 8** Electrostatic potential surface of the most stable conformers of the cores of systems **I**, **II** and **III** (blue to red colour – positive to negative part of molecule)

**Table 2** Relative energies, bending angles, dipole moment components ( $\mu_x$ ,  $\mu_y$ ,  $\mu_z$ ) and modulus ( $\mu$ ) of the investigated five-ring systems

Conformer	Energy (kcal)	Dipole moment (Debye)				Bending angle (°)		
		$\mu$	$\mu_x$	$\mu_y$	$\mu_z$	$\alpha_1$	$\alpha_2$	$\alpha^a$
<b>IA</b>	0.0	12.05	0.00	11.57	-3.38	117.0 <sup>b</sup>	97.0	107.0
<b>IB</b>	16.42	0.48	0.00	0.48	0.00	106.5	115.3	110.9
<b>IC</b>	6.60	6.18	4.21	-4.46	0.84	113.0	110.4	111.7
<b>IIA</b>	0.0	1.15	0.50	-0.42	0.95	83.1	75.5	79.3
<b>IIB</b>	3.57	4.13	0.0	4.01	1.01	150.0	155.0	152.75
<b>IIC</b>	1.51	3.16	2.72	1.60	-0.04	115.12	112.4	113.75
<b>IIIA</b>	0.0	1.82	0.0	-1.63	-0.80	94.3 <sup>c</sup>	98.9	96.6
<b>IIIB</b>	2.38	2.64	0.0	-2.49	-0.87	131.0	124.6	127.8
<b>IIIC</b>	1.03	2.11	-0.32	-2.08	0.06	112.24	111.0	111.6

<sup>a</sup>  $\alpha = (\alpha_1 + \alpha_2)/2$

<sup>b</sup> Bending angle for *N,N'*-dibenzoyl-2,6-diaminopyridine<sup>27</sup> is 123.5°

<sup>c</sup> Bending angle for 2,6-dibenzylidene-pyridine<sup>28</sup> is 95.3°



For the system **II** there is no adequate compound in the Cambridge Structural Database<sup>29</sup> for comparison, while 2,6-dibenzylidene pyridine<sup>28</sup> has a bending angle of 95.3° which is almost the same as obtained for the most stable conformer **IIIA** (94.3°). When compared to reported bending angles of bent-core liquid crystals containing benzene as central unit,<sup>24</sup> the bending angles of the investigated systems are narrow and it might be a reason the higher homologues form B7 mesophase.

DFT results demonstrate that the main contribution to the dipole moment of the systems **I** and **III** is due to the  $\mu_y$  component. This is in agreement with the observation of Rama Krishnan *et al.*<sup>24</sup>, who found that for small total dipole moments,  $\mu_y$  yields the major contribution to  $\mu$ , and the formation of smectic phase is favoured.

## Conclusions

We have synthesized and characterized three series of bent-core mesogens having pyridine as central unit. The phases have been characterized by optical microscopy observations, differential scanning calorimetry (DSC) and confirmed by X-ray studies. A series **I** of 2,6-diaminopyridine derivatives capable to form inter- and intramolecular hydrogen bonds exhibits very high melting points and do not show mesomorphism. A decrease in the polarity of the central part of the bent-core achieved by replacing the amide with ester linkages results in derivatives (series **II**) with lower melting points and a formation of a very short undefined mesophase. The introduction of the olefinic groups, which connect the pyridine ring with the inner aromatic rings (series **III**), helps to further lower the polarity of the central part in the five ring system and led to the formation of a columnar (B1) phase in **IIIb** and a layer modulated smectic CP (B7) phases in case of **IIIc**. For this latter material the layer spacing and the modulation periodicities have been determined at the function of the temperature by small angle synchrotron x-ray measurements. The bending angles and polarity of the investigated five-ring systems have been calculated by density functional theory (DFT) method.

These results will guide the design and synthesis of new pyridine based bent-core liquid crystals with lower and wider mesophase ranges.

## Experimental

### Synthetic procedures

The reagents were purchased from Sigma Aldrich and were used without further purifications. All solvents were dried and distilled using general standard procedures. The chemical structures and the purities of the synthesized compounds were confirmed by melting points, elemental analysis, FT-IR, <sup>1</sup>H and <sup>13</sup>C NMR spectra.

*Preparation of N,N'-bis[4-(4-alkyloxyphenyl)methyliminobenzoyl]-2,6-diaminopyridines (Ia-Ic)*

*N,N'-Bis(4-aminobenzoyl)-2,6-diaminopyridine (Id)*. A mixture of *N,N'*-bis(4-nitrobenzoyl)-2,6-diaminopyridine (**1c**, 8.00 g, 19.7 mmol) and 180 cm<sup>3</sup> of 70 % acetic acid was hydrogenated with 4.36 g of 5% Pd/C at 25 °C for 5 h. After filtration and evaporation, the product was suspended in 100 cm<sup>3</sup> of an aqueous solution of NaHCO<sub>3</sub> and stirred for 90 min.

The solid was filtered off and rinsed with plenty of water (yield 48.5 %). The melting points, FT-IR, <sup>1</sup>H and <sup>13</sup>C NMR spectra of compound **Id** are in agreement with literature data and undoubtedly corroborate their structures.

*N,N'-Bis[4-(4-alkyloxyphenyl)methyliminobenzoyl]-2,6-diaminopyridines (Ia-Ic)*. To the solution of *N,N'*-bis(4-aminobenzoyl)-2,6-diaminopyridine (**1d**) (3.00 mmol) in dimethyl sulfoxide (20 cm<sup>3</sup>) was added dropwise a solution of respective 4-*n*-alkoxybenzaldehyde (**1e-1g**) (6.00 mmol) in DMSO (10 cm<sup>3</sup>). The reaction was carried out at 90 °C for 24h. After cooling to the room temperature, ethanol was added dropwise and separated precipitate was filtered off and recrystallized from toluene.

*N,N'-Bis[4-(4-pentyloxyphenyl)methyliminobenzoyl]-2,6-diaminopyridine (Ia)* Yield 49 %; FTIR (KBr)  $\nu$  = 3328, 2933, 2860, 1650, 1592, 1509, 1460, 1307, 1254, 1163, 848, 833, 794 cm<sup>-1</sup>; <sup>1</sup>H NMR (500 MHz, CDCl<sub>3</sub>):  $\delta$  0.95 (t,  $J$  = 7.0 Hz, 6H, CH<sub>3</sub>), 1.38-1.50 (m, 8H, CH<sub>2</sub>), 1.83 (quin,  $J$  = 7.0 Hz, 4H, CH<sub>2</sub>), 4.03 (t,  $J$  = 6.5 Hz, 4H, CH<sub>2</sub>), 6.99 (d,  $J$  = 9.0 Hz, 4H, Ar), 7.26 (d,  $J$  = 8.5 Hz, 4H, Ar), 7.82 (t,  $J$  = 8.0 Hz, 1H, Py), 7.85 (d,  $J$  = 8.5 Hz, 4H, Ar), 7.95 (d,  $J$  = 8.5 Hz, 4H, Ar), 8.12 (d,  $J$  = 8.0 Hz, 2H, Py), 8.37 (s, 2H, CH=N), 8.38 (s, 2H, NH-C=O) ppm; <sup>13</sup>C NMR (125 MHz, CDCl<sub>3</sub>):  $\delta$  13.99 (CH<sub>3</sub>), 22.43 (CH<sub>2</sub>), 28.14 (CH<sub>2</sub>), 28.83 (CH<sub>2</sub>), 68.25 (CH<sub>2</sub>), 109.8 (Py), 114.8 (Ar), 121.2 (Ar), 128.4 (Ar), 128.5 (Ar), 130.7 (Ar), 130.9 (Ar), 141.0 (Py), 149.8 (Ar), 156.1 (Py), 161.1 (CH=N), 162.4 (Ar), 165.0 (C=O) ppm. Elemental analysis, found: C, 73.93; H, 6.44; N, 9.97. Calc. for C<sub>43</sub>H<sub>45</sub>N<sub>5</sub>O<sub>4</sub>: C, 74.22; H, 6.52; N, 10.06%.

*N,N'-Bis[4-(4-heptyloxyphenyl)methyliminobenzoyl]-2,6-diaminopyridine (Ib)* Yield 51 %; FTIR (KBr)  $\nu$  = 3325, 2925, 2855, 1650, 1590, 1509, 1459, 1305, 1252, 1162, 847, 833, 794 cm<sup>-1</sup>; <sup>1</sup>H NMR (500 MHz, CDCl<sub>3</sub>):  $\delta$  0.90 (t,  $J$  = 7.0 Hz, 6H, CH<sub>3</sub>), 1.32-1.50 (m, 16H, CH<sub>2</sub>), 1.82 (quin,  $J$  = 7.0 Hz, 4H, CH<sub>2</sub>), 4.03 (t,  $J$  = 6.5 Hz, 4H, CH<sub>2</sub>), 6.98 (d,  $J$  = 9.0 Hz, 4H, Ar), 7.26 (d,  $J$  = 8.5 Hz, 4H, Ar), 7.82 (t,  $J$  = 8.0 Hz, 1H, Py), 7.85 (d,  $J$  = 8.5 Hz, 4H, Ar), 7.94 (d,  $J$  = 8.5 Hz, 4H, Ar), 8.12 (d,  $J$  = 8.0 Hz, 2H, Py), 8.34 (s, 2H, CH=N), 8.37 (s, 2H, NH-C=O) ppm; <sup>13</sup>C NMR (125 MHz, CDCl<sub>3</sub>):  $\delta$  14.06 (CH<sub>3</sub>), 22.59 (CH<sub>2</sub>), 25.95 (CH<sub>2</sub>), 29.02 (CH<sub>2</sub>), 29.14 (CH<sub>2</sub>), 31.75 (CH<sub>2</sub>), 68.27 (CH<sub>2</sub>), 109.7 (Py), 114.8 (Ar), 121.2 (Ar), 128.4 (Ar), 128.5 (Ar), 130.7 (Ar), 130.9 (Ar), 141.0 (Py), 149.8 (Ar), 156.1 (Py), 161.1 (CH=N), 162.4 (Ar), 165.0 (C=O) ppm. Elemental analysis, found: C, 74.80; H, 7.01; N, 9.22. Calc. for C<sub>47</sub>H<sub>53</sub>N<sub>5</sub>O<sub>4</sub>: C, 75.07; H, 7.10; N, 9.31%.

*N,N'-Bis[4-(4-dodecyloxyphenyl)methyliminobenzoyl]-2,6-diaminopyridine (Ic)* Yield 47 %; FTIR (KBr)  $\nu$  = 3293, 2919, 2851, 1648, 1590, 1509, 1462, 1305, 1249, 1167, 852, 796 cm<sup>-1</sup>; <sup>1</sup>H NMR (500 MHz, CDCl<sub>3</sub>):  $\delta$  0.88 (t,  $J$  = 7.5 Hz, 6H, CH<sub>3</sub>), 1.27-1.50 (m, 36H, CH<sub>2</sub>), 1.82 (quin,  $J$  = 7.0 Hz, 4H, CH<sub>2</sub>), 4.04 (t,  $J$  = 6.5 Hz, 4H, CH<sub>2</sub>), 6.99 (d,  $J$  = 9.0 Hz, 4H, Ar), 7.27 (d,  $J$  = 9.0 Hz, 4H, Ar), 7.83 (t,  $J$  = 8.5 Hz, 1H, Py), 7.86 (d,  $J$  = 9.0 Hz, 4H, Ar), 7.95 (d,  $J$  = 8.5 Hz, 4H, Ar), 8.13 (d,  $J$  = 8.0 Hz, 2H, Py), 8.32 (s, 2H, CH=N), 8.38 (s, 2H, NH-C=O) ppm; <sup>13</sup>C NMR (125 MHz, CDCl<sub>3</sub>):  $\delta$  14.11 (CH<sub>3</sub>), 22.68 (CH<sub>2</sub>), 25.99 (CH<sub>2</sub>), 29.15 (CH<sub>2</sub>), 29.34 (CH<sub>2</sub>), 29.37 (CH<sub>2</sub>), 29.55 (CH<sub>2</sub>), 29.58 (CH<sub>2</sub>), 29.63 (CH<sub>2</sub>), 29.65 (CH<sub>2</sub>), 31.91 (CH<sub>2</sub>), 68.29 (CH<sub>2</sub>), 109.7 (Py), 114.8 (Ar), 121.2 (Ar), 128.4 (Ar), 128.5 (Ar), 130.8 (Ar), 130.9 (Ar), 141.0 (Py), 149.8 (Ar), 156.2 (Py), 161.1 (CH=N), 162.4 (Ar), 165.0 (C=O) ppm.

Elemental analysis, found: C, 76.43; H, 8.16; N, 7.78. Calc. for  $C_{57}H_{73}N_3O_4$ : C, 76.73; H, 8.25; N, 7.85%.

*Preparation of di[4-(4-n-alkoxyphenyliminomethyl)phenyl]pyridine-2,6-dicarboxylates (IIa-IIIc)*

*Di(4-formylphenyl)pyridine-2,6-dicarboxylate (2d)*. To an ice-cold solution of 4-hydroxybenzaldehyde (**2c**, 20.8 g, 0.171 mol) in dry pyridine (100  $cm^3$ ) was added gradually a dipicolinic acid chloride (**2b**, 17.6 g, 0.095 mol). The reaction mixture was stirred at room temperature for 2 days, solvent was removed under reduced pressure, and the residue was rinsed with plenty of water. The crude product was purified by recrystallization from dimethylformamide, and the obtained yield was 62%. m.p.=220-222 °C; FTIR (KBr)  $\nu$  = 3063, 1761, 1683, 1597, 1573, 1395, 1308, 1233, 1208, 1171, 1156, 995, 907, 831, 752, 727, 565, 417  $cm^{-1}$ ;  $^1H$  NMR (200 MHz,  $CDCl_3$ ):  $\delta$  7.62 (d,  $J$  = 8.4 Hz, 4H, Ar), 8.07 (d,  $J$  = 8.6 Hz, 4H, Ar), 8.39 (t,  $J$  = 7.8 Hz, 1H, Py), 8.58 (d,  $J$  = 7.8 Hz, 2H, Py), 10.05 (s, 2H, CHO) ppm;  $^{13}C$  NMR (50 MHz,  $CDCl_3$ ):  $\delta$  123.1(Ar), 129.9 (Py), 131.5 (Ar), 134.6 (Ar), 140.1 (Py), 147.2 (Py), 155.4 (Ar), 162.6 (COO), 192.4 (CHO) ppm. Elemental analysis, found: C, 66.94; H, 3.53; N, 3.70. Calc. for  $C_{21}H_{13}NO_6$ : C, 67.20; H, 3.49; N, 3.73%.

*Di[4-(4-n-alkoxyphenyliminomethyl)phenyl]pyridine-2,6-dicarboxylates (IIa-IIIc)*. To the solution of di(4-formylphenyl)pyridine-2,6-dicarboxylate (**2d**) (3.00 mmol) in dimethyl sulfoxide (35  $cm^3$ ) was added dropwise a solution of respective 4-n-alkoxyaniline (**2e-2g**) (6.00 mmol) in DMSO (15  $cm^3$ ). The reaction was carried out at 90 °C for 24 h. After cooling to the room temperature, precipitate was filtered off and recrystallized from toluene.

*Di[4-(4-n-pentoxyphenyliminomethyl)phenyl]pyridine-2,6-dicarboxylate (IIa)* Yield 54 %; FTIR (KBr)  $\nu$  = 3067, 2957, 2937, 2864, 1762, 1624, 1604, 1578, 1508, 1253, 1230, 1161, 1022, 867, 836, 553  $cm^{-1}$ ;  $^1H$  NMR (500 MHz,  $CDCl_3$ ):  $\delta$  0.91 (t,  $J$  = 7.0 Hz, 6H,  $CH_3$ ), 1.37-1.48 (m, 8H,  $CH_2$ ), 1.86 (quin,  $J$  = 7.0 Hz, 4H,  $CH_2$ ), 4.16 (t,  $J$  = 6.5 Hz, 4H,  $CH_2$ ), 7.17 (d,  $J$  = 9.0 Hz, 4H, Ar), 7.68 (d,  $J$  = 9.5 Hz, 4H, Ar), 7.76 (d,  $J$  = 8.5 Hz, 4H, Ar), 8.33 (d,  $J$  = 9.0 Hz, 4H, Ar), 8.84 (t,  $J$  = 8.0 Hz, 1H, Py), 8.97 (d,  $J$  = 8.0 Hz, 2H, Py), 9.13 (s, 2H, CH=N) ppm;  $^{13}C$  NMR (125 MHz,  $CDCl_3$ ):  $\delta$  14.50 ( $CH_3$ ), 24.07 ( $CH_2$ ), 29.79 ( $CH_2$ ), 30.38 ( $CH_2$ ), 72.13 ( $CH_2$ ), 119.1 (Ar), 124.6 (Ar), 125.6 (Ar), 127.8 (Py), 131.1 (Ar), 133.8 (Ar), 136.3 (Ar), 145.9 (Ar), 148.8 (Py), 159.6 (Py), 161.2 (Ar), 163.3 (C=O), 164.6 (CH=N) ppm. Elemental analysis, found: C, 73.73; H, 6.14; N, 5.95. Calc. for  $C_{43}H_{43}N_3O_6$ : C, 74.01; H, 6.21; N, 6.02%.

*Di[4-(4-n-heptyloxyphenyliminomethyl)phenyl]pyridine-2,6-dicarboxylate (IIb)* Yield 49 %; FTIR (KBr)  $\nu$  = 3068, 2953, 2935, 2858, 1762, 1623, 1604, 1578, 1508, 1254, 1231, 1162, 1148, 867, 835, 554  $cm^{-1}$ ;  $^1H$  NMR (500 MHz,  $CDCl_3$ ):  $\delta$  0.85 (t,  $J$  = 7.0 Hz, 6H,  $CH_3$ ), 1.28-1.51 (m, 16H,  $CH_2$ ), 1.85 (quin,  $J$  = 7.0 Hz, 4H,  $CH_2$ ), 4.16 (t,  $J$  = 6.5 Hz, 4H,  $CH_2$ ), 7.16 (d,  $J$  = 9.0 Hz, 4H, Ar), 7.68 (d,  $J$  = 9.5 Hz, 4H, Ar), 7.75 (d,  $J$  = 9.0 Hz, 4H, Ar), 8.32 (d,  $J$  = 8.5 Hz, 4H, Ar), 8.83 (t,  $J$  = 8.0 Hz, 1H, Py), 8.96 (d,  $J$  = 8.0 Hz, 2H, Py), 9.12 (s, 2H, CH=N) ppm;  $^{13}C$  NMR (125 MHz,  $CDCl_3$ ):  $\delta$  14.69 ( $CH_3$ ), 24.35 ( $CH_2$ ), 27.62 ( $CH_2$ ), 30.71 ( $CH_2$ ), 30.86 ( $CH_2$ ), 33.69 ( $CH_2$ ), 72.19 ( $CH_2$ ), 119.1 (Ar), 124.6 (Ar), 125.6 (Ar), 127.8 (Py), 131.2

(Ar), 133.8 (Ar), 136.4 (Ar), 146.0 (Ar), 148.8 (Py), 159.6 (Py), 161.2 (Ar), 163.3 (C=O), 164.6 (CH=N) ppm. Elemental analysis, found: C, 74.61; H, 6.74; N, 5.52. Calc. for  $C_{47}H_{51}N_3O_6$ : C, 74.88; H, 6.82; N, 5.57%.

*Di[4-(4-n-dodecyloxyphenyliminomethyl)phenyl]pyridine-2,6-dicarboxylate (IIc)* Yield 57 %; FTIR (KBr)  $\nu$  = 3070, 2956, 2919, 2850, 1762, 1624, 1605, 1578, 1509, 1253, 1162, 1024, 867, 836, 554  $cm^{-1}$ ;  $^1H$  NMR (500 MHz,  $CDCl_3$ ):  $\delta$  0.83 (t,  $J$  = 7.0 Hz, 6H,  $CH_3$ ), 1.27-1.52 (m, 36H,  $CH_2$ ), 1.86 (quin,  $J$  = 7.0 Hz, 4H,  $CH_2$ ), 4.16 (t,  $J$  = 6.5 Hz, 4H,  $CH_2$ ), 7.16 (d,  $J$  = 9.0 Hz, 4H, Ar), 7.68 (d,  $J$  = 9.0 Hz, 4H, Ar), 7.75 (d,  $J$  = 9.0 Hz, 4H, Ar), 8.32 (d,  $J$  = 9.0 Hz, 4H, Ar), 8.83 (t,  $J$  = 8.0 Hz, 1H, Py), 8.96 (d,  $J$  = 8.0 Hz, 2H, Py), 9.12 (s, 2H, CH=N) ppm;  $^{13}C$  NMR (125 MHz,  $CDCl_3$ ):  $\delta$  14.75 ( $CH_3$ ), 24.45 ( $CH_2$ ), 27.61 ( $CH_2$ ), 30.67 ( $CH_2$ ), 31.14 ( $CH_2$ ), 31.28 ( $CH_2$ ), 31.40 ( $CH_2$ ), 31.46 ( $CH_2$ ), 31.54 ( $CH_2$ ), 33.89 ( $CH_2$ ), 72.15 ( $CH_2$ ), 119.1 (Ar), 124.6 (Ar), 125.6 (Ar), 127.7 (Py), 131.1 (Ar), 133.8 (Ar), 136.3 (Ar), 145.9 (Ar), 148.7 (Py), 159.6 (Py), 161.2 (Ar), 163.2 (C=O), 164.6 (CH=N) ppm. Elemental analysis, found: C, 76.32; H, 7.92; N, 4.64. Calc. for  $C_{57}H_{71}N_3O_6$ : C, 76.56; H, 8.00; N, 4.70%.

*Preparation of 2,6-bis[2-(4-(4-alkoxybenzoyloxy)phenyl)ethenyl]pyridines (IIIa-IIIc)*

*2,6-Bis[2-(4-hydroxyphenyl)ethenyl]pyridine (3c)* was synthesized by modifying a literature procedure.<sup>15</sup> A mixture of 2,6-lutidine (**3a**, 2.7 g, 0.025 mol), 4-hydroxybenzaldehyde (**2c**, 9.2 g, 0.075 mol) and acetic anhydride (25  $cm^3$ ) was refluxed for 24 hours at 155 °C. The reaction mixture was poured into cold water (150  $cm^3$ ) and shaking until the excess acetic anhydride was completely hydrolyzed. The product was filtered, washed with water and recrystallized repeatedly from ethanol. A mixture of obtained 2,6-bis-[2-(4-ethanoyloxyphenyl)ethenyl]pyridine (**3b**, 1.5 g) and 0.75 mol  $dm^{-3}$  alcoholic potassium hydroxide (15  $cm^3$ ) was refluxed for ninety minutes and the reaction product precipitated from the clear solution as a voluminous powder by a current of carbon dioxide. 2,6-Bis[2-(4-hydroxyphenyl)ethenyl]pyridine (**3c**) was recrystallized from ethanol. Yield 32 %; m.p.>300 °C; FTIR (KBr)  $\nu$  = 3252, 1632, 1604, 1582, 1559, 1512, 1458, 1254, 1208, 1173, 1004, 955, 830, 820, 801, 781, 740, 518  $cm^{-1}$ ;  $^1H$  NMR (200 MHz,  $CDCl_3$ ):  $\delta$  6.82 (d,  $J$  = 8.6 Hz, 4H, Ar), 7.09 (d,  $J$  = 16.2 Hz, 2H, CH=CH), 7.31(d,  $J$  = 7.6 Hz, 2H, Py), 7.53 (d,  $J$  = 8.4 Hz, 4H, Ar), 7.67 (d,  $J$  = 15.8 Hz, 2H, CH=CH), 7.69 (t,  $J$  = 7.7 Hz, 1H, Py), 9.71 (s, 2H, OH) ppm;  $^{13}C$  NMR (50 MHz,  $CDCl_3$ ):  $\delta$  115.9 (Ar), 120.1 (Py), 125.3 (CH=CH), 127.8 (Ar), 128.8 (Ar), 132.5 (CH=CH), 137.4 (Py), 155.4 (Py), 158.2 (Ar) ppm. Elemental analysis, found: C, 79.69; H, 5.47; N, 4.39. Calc. for  $C_{21}H_{17}NO_2$ : C, 79.98; H, 5.43; N, 4.44%.

*2,6-Bis[2-(4-(4-alkoxybenzoyloxy)phenyl)ethenyl]pyridines (IIIa-IIIc)*. To an ice-cold solution of 2,6-bis[2-(4-hydroxyphenyl)ethenyl]pyridine (**3c**) (3.00 mmol) in dry pyridine (30  $cm^3$ ) was added slowly respective 4-n-alkoxybenzoyl chloride (**3g-3i**) (6.00 mmol). The reaction was carried out at room temperature for 2 days. The product was filtered off and recrystallized from acetone and toluene successively.

*2,6-Bis[2-(4-(4-pentoxybenzoyloxy)phenyl)ethenyl]pyridine (IIIa)* Yield 46 %; FTIR (KBr)  $\nu$  = 2957, 2935, 2860, 1728,

1606, 1579, 1561, 1510, 1458, 1276, 1256, 1212, 1164, 1069, 762 cm<sup>-1</sup>; <sup>1</sup>H NMR (500 MHz, CDCl<sub>3</sub>): δ 0.95 (t, *J* = 7.0 Hz, 6H, CH<sub>3</sub>), 1.38-1.50 (m, 8H, CH<sub>2</sub>), 1.83 (quin, *J* = 7.0 Hz, 4H, CH<sub>2</sub>), 4.04 (t, *J* = 6.5 Hz, 4H, CH<sub>2</sub>), 6.97 (d, *J* = 9.0 Hz, 4H, Ar), 7.18 (d, *J* = 16.0 Hz, 2H, CH=CH), 7.24 (d, *J* = 8.5 Hz, 4H, Ar), 7.27 (d, *J* = 7.5 Hz, 2H, Py), 7.64 (t, *J* = 8.0 Hz, 1H, Py), 7.66 (d, *J* = 8.5 Hz, 4H, Ar), 7.73 (d, *J* = 16.0 Hz, 2H, CH=CH), 8.15 (d, *J* = 8.5 Hz, 4H, Ar) ppm; <sup>13</sup>C NMR (125 MHz, CDCl<sub>3</sub>): δ 13.98 (CH<sub>3</sub>), 22.41 (CH<sub>2</sub>), 28.11 (CH<sub>2</sub>), 28.77 (CH<sub>2</sub>), 68.30 (CH<sub>2</sub>), 114.3 (Ar), 120.5 (Ar), 121.4 (Py), 122.1 (Ar), 128.1 (Ar), 128.3 (CH=CH), 132.0 (CH=CH), 132.3 (Ar), 134.4 (Ar), 137.0 (Py), 151.0 (Ar), 155.3 (Py), 163.6 (Ar), 164.8 (C=O) ppm. Elemental analysis, found: C, 77.41; H, 6.48; N, 1.98. Calc. for C<sub>45</sub>H<sub>45</sub>NO<sub>6</sub>: C, 77.67; H, 6.52; N, 2.01%.

**2,6-Bis[2-(4-(4-heptyloxybenzoyloxy)phenyl)ethenyl]pyridine (IIIb)** Yield 43 %; FTIR (KBr)  $\nu$  = 2929, 2856, 1727, 1606, 1579, 1562, 1510, 1460, 1257, 1212, 1164, 1073, 762 cm<sup>-1</sup>; <sup>1</sup>H NMR (500 MHz, CDCl<sub>3</sub>): δ 0.90 (t, *J* = 7.0 Hz, 6H, CH<sub>3</sub>), 1.32-1.50 (m, 16H, CH<sub>2</sub>), 1.82 (quin, *J* = 7.0 Hz, 4H, CH<sub>2</sub>), 4.04 (t, *J* = 6.5 Hz, 4H, CH<sub>2</sub>), 6.97 (d, *J* = 8.5 Hz, 4H, Ar), 7.18 (d, *J* = 16.0 Hz, 2H, CH=CH), 7.24 (d, *J* = 8.5 Hz, 4H, Ar), 7.27 (d, *J* = 7.5 Hz, 2H, Py), 7.64 (t, *J* = 7.5 Hz, 1H, Py), 7.66 (d, *J* = 8.5 Hz, 4H, Ar), 7.73 (d, *J* = 16.5 Hz, 2H, CH=CH), 8.15 (d, *J* = 9.0 Hz, 4H, Ar) ppm; <sup>13</sup>C NMR (125 MHz, CDCl<sub>3</sub>): δ 14.06 (CH<sub>3</sub>), 22.58 (CH<sub>2</sub>), 25.92 (CH<sub>2</sub>), 29.01 (CH<sub>2</sub>), 29.08 (CH<sub>2</sub>), 31.73 (CH<sub>2</sub>), 68.32 (CH<sub>2</sub>), 114.3 (Ar), 120.5 (Ar), 121.4 (Py), 122.1 (Ar), 128.1 (Ar), 128.3 (CH=CH), 132.0 (CH=CH), 132.3 (Ar), 134.4 (Ar), 137.0 (Py), 151.0 (Ar), 155.3 (Py), 163.6 (Ar), 164.8 (C=O) ppm. Elemental analysis, found: C, 78.02; H, 7.04; N, 1.84. Calc. for C<sub>49</sub>H<sub>53</sub>NO<sub>6</sub>: C, 78.27; H, 7.10; N, 1.86%.

**2,6-Bis[2-(4-(4-dodecyloxybenzoyloxy)phenyl)ethenyl]pyridine (IIIc)** Yield 51 %; FTIR (KBr)  $\nu$  = 2956, 2919, 2850, 1726, 1609, 1579, 1564, 1509, 1459, 1288, 1253, 1212, 1196, 1170, 761 cm<sup>-1</sup>; <sup>1</sup>H NMR (500 MHz, CDCl<sub>3</sub>): δ 0.89 (t, *J* = 7.0 Hz, 6H, CH<sub>3</sub>), 1.27-1.50 (m, 36H, CH<sub>2</sub>), 1.82 (quin, *J* = 7.0 Hz, 4H, CH<sub>2</sub>), 4.04 (t, *J* = 6.5 Hz, 4H, CH<sub>2</sub>), 6.97 (d, *J* = 9.0 Hz, 4H, Ar), 7.18 (d, *J* = 16.0 Hz, 2H, CH=CH), 7.24 (d, *J* = 8.5 Hz, 4H, Ar), 7.27 (d, *J* = 7.5 Hz, 2H, Py), 7.64 (t, *J* = 7.5 Hz, 1H, Py), 7.66 (d, *J* = 8.5 Hz, 4H, Ar), 7.73 (d, *J* = 16.5 Hz, 2H, CH=CH), 8.15 (d, *J* = 9.0 Hz, 4H, Ar) ppm; <sup>13</sup>C NMR (125 MHz, CDCl<sub>3</sub>): δ 14.10 (CH<sub>3</sub>), 22.67 (CH<sub>2</sub>), 25.97 (CH<sub>2</sub>), 29.08 (CH<sub>2</sub>), 29.34 (CH<sub>2</sub>), 29.35 (CH<sub>2</sub>), 29.54 (CH<sub>2</sub>), 29.57 (CH<sub>2</sub>), 29.62 (CH<sub>2</sub>), 29.64 (CH<sub>2</sub>), 31.90 (CH<sub>2</sub>), 68.33 (CH<sub>2</sub>), 114.3 (Ar), 120.5 (Ar), 121.4 (Py), 122.1 (Ar), 128.1 (Ar), 128.3 (CH=CH), 132.0 (CH=CH), 132.3 (Ar), 134.4 (Ar), 137.0 (Py), 151.0 (Ar), 155.3 (Py), 163.6 (Ar), 164.9 (C=O) ppm. Elemental analysis, found: C, 79.15; H, 8.20; N, 1.56. Calc. for C<sub>59</sub>H<sub>73</sub>NO<sub>6</sub>: C, 79.42; H, 8.25; N, 1.57%.

### Physical investigations

To confirm the chemical structure of the synthesized compounds the following analytical methods were applied. Fourier-transform infrared spectra (FT-IR) were recorded on a Bomem MB 100 spectrophotometer ( $\nu_{\max}$  in cm<sup>-1</sup>) on KBr pellets. <sup>1</sup>H and <sup>13</sup>C nuclear magnetic resonance (NMR) spectra were recorded on a Varian Gemini 200 spectrometer on 200 MHz or Bruker AVANCE on 500 MHz, whereas <sup>13</sup>C spectra were recorded on 50 or 125 MHz. NMR spectra were recorded in CDCl<sub>3</sub>, or DMSO-*d*<sub>6</sub>, using TMS as the internal standard (chemical shift  $\delta$  in ppm). Elemental analysis was realized

using an Elemental Vario EL III microanalyzer, their results were found to be in good agreement ( $\pm 0.3\%$ ) with the calculated values.

The temperatures and enthalpies of the phase transitions were determined by differential scanning calorimetry (DSC) on METTLER FP89 using cooling and heating runs at a rate of 5°C min<sup>-1</sup>. The samples of 3–5 mg were sealed in aluminium pans.

For electro-optical investigations the materials were filled in home made 5  $\mu$ m thick films with transparent indium tin oxide (ITO) electrodes and antiparallel rubbed polyimide alignment layer. The electro-optical measurements were done using an Olympus BX51 microscope equipped with 90° crossed polarizers, an HCS402 hot stage from Instec Inc., and a digital camera (14.2 Mp Color Mosaic Model from Diagnostic Instruments, Inc.). The images were captured using a Hitachi CCD camera under transmitted light between crossed polarizers. The electric signals were applied by a HP function generator and FLC voltage amplifier.

Small angle x-ray scattering (SAXS) measurements were performed at the National Synchrotron Light Source (NSLS, beam line X6B) of Brookhaven National Lab. The materials were filled into 1 mm diameter quartz x-ray tubes, which were then mounted into a custom-built aluminum cassette that allowed x-ray detection with  $\pm 13.5^\circ$  angular range. The cassette fits into a standard hot stage (Instec model HCS402) that allowed temperature control with  $\pm 0.05^\circ\text{C}$  precision. The stage also included two cylindrical neodymium iron boron magnets that supplied a magnetic induction of  $B=1.5\text{T}$  perpendicular to the incident x-ray beam. Two-dimensional SAXS images were recorded on a Princeton Instruments 2084  $\times$  2084 pixel array CCD detector. The beamline was configured for a collimated beam (0.2mm  $\times$  0.3 mm) at energy 16 keV (0.775 Å). Details of the experimental conditions are described elsewhere.<sup>30</sup>

### Computational details

The information related to molecular conformation, bending angle and dipole moment of the investigated mesogens were elucidated by the density functional theory (DFT) using the 6–311G(d,p) basis set. All calculations were done with Gaussian03 software.<sup>31</sup>

### Acknowledgements

The authors are grateful to the Ministry of Education, Science and Technological Development of the Republic of Serbia, Project No. 172013, and Hungarian Research Fund, Contract No. OTKA-K81250, for financial support.

### Notes and references

<sup>a</sup> Faculty of Technology and Metallurgy, University of Belgrade, Belgrade, Serbia.

<sup>b</sup> Wigner Research Centre for Physics, Institute for Solid State Physics and Optics of the Hungarian Academy of Sciences H-1525 Budapest, P.O.Box 49, Hungary.

<sup>c</sup> Faculty of Chemistry, University of Belgrade, Belgrade, Serbia.

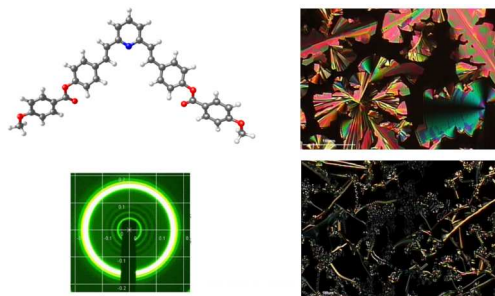
<sup>d</sup> Liquid Crystal Institute, Kent State University, Kent, Ohio 44242, USA.

† Electronic Supplementary Information (ESI) available: [details of any supplementary information available should be included here]. See DOI: 10.1039/b000000x/



- 1 G. Decher, B. Tieke, C. Bosshard and P. Günter, *Ferroelectrics*, 1989, **91**, 193.
- 2 L. Mutter, F. D. J. Brunner, Z. Yang, M. Jazbinšek and P. Günter, *J. Opt. Soc. Am. B*, 2007, **24**, 2556.
- 3 H. Kang, A. Facchetti, H. Jiang, E. Cariati, S. Righetto, R. Ugo, C. Zuccaccia, A. Macchioni, C. L. Stern, Z. Liu, S.-T. Ho, E. C. Brown, M. A. Ratner and T. J. Marks, *J. Am. Chem. Soc.*, 2007, **129**, 3267.
- 4 A.-J. Attias, C. Cavalli, B. Bloch, N. Guillou and C. Noël, *Chem. Mater.*, 1999, **11**, 2057.
- 5 A. Eremin and A. Jákli, *Soft Matter*, 2013, **9**, 615.
- 6 G. Heppke, A. Jákli, S. Rauch and H. Sawade, *Phys. Rev. E*, 1999, **60**, 5575.
- 7 D. Shen, S. Diele, G. Pelzl, I. Wirth and C. Tschierske, *J. Mater. Chem.*, 1999, **9**, 661.
- 8 J. Matraszek, J. Mieczkowski, J. Szydłowska and E. Gorecka, *Liq. Cryst.*, 2000, **27**, 429.
- 9 G. Pelzl, S. Diele and W. Weissflog, *Adv. Mater.*, 1999, **11**, 707.
- 10 A. Pérez, N. Gimeno, F. Vera, M. B. Ros, J. L. Serrano and M. R. De la Fuente, *Eur. J. Org. Chem.*, 2008, **2008**, 826.
- 11 M. Alaasar, C. Tschierske and M. Prehm, *Liq. Cryst.*, 2011, **38**, 925–934.
- 12 A. Gamliel, M. Afri and A. A. Frimer, *Free Radical Bio. Med.*, 2008, **44**, 1394.
- 13 P. Langer, S. Amiri, A. Bodtke, N. N. R. Saleh, K. Weisz, H. Görls and P. R. Schreiner, *J. Org. Chem.*, 2008, **73**, 5048.
- 14 B. T. Thaker, B. S. Patel, D. B. Solanki, Y. T. Dhimmer and J. S. Dave, *Mol. Cryst. Liq. Cryst.*, 2010, **517**, 63.
- 15 E. D. Bergmann and S. Pinchas, *J. Org. Chem.*, 1950, **15**, 1184.
- 16 S. Kutsumizu, H. Mori, M. Fukatami, S. Naito, K. Sakajiri and K. Saito, *Chem. Mater.*, 2008, **20**, 3675.
- 17 H. Takezoe and Y. Takanishi, *Jpn. J. Appl. Phys., Part 1*, 2006, **45**, 597.
- 18 K. Gomola, L. Guo, D. Pocięcha, F. Araoka, K. Ishikawa and H. Takezoe, *J. Mater. Chem.*, 2010, **20**, 7944.
- 19 V. Kozmík, M. Horčic, J. Svoboda, V. Novotná and D. Pocięcha, *Liq. Cryst.*, 2012, **39**, 943.
- 20 J. Thisayukta, Y. Nakayama and J. Watanabe, *Liq. Cryst.*, 2000, **27**, 1129.
- 21 D.A. Coleman, J. Fernsler, N. Chattham, M. Nakata, Y. Takanishi, E. Ko, D.R. Link, R.R.-F. Shao, W.G. Jang, J.E. MacLennan, C. Boyer, W. Weissflog, G. Pelzl, L.-C. Chien, J.A.N. Zasadzinski, J. Watanabe, D.M. Walba, H. Takezoe, and N. A. Clark, *Science*, 2003, **301**, 1204.
- 22 C. Zhang, N. Diorio, S. Radhika, B.K. Sadashiva, S.N. Sprunt, and A. Jákli, *Liq. Cryst.*, 2012, **39**, 1149.
- 23 N. Vaupotič, M. Čopič, E. Gorecka, D. Pocięcha, *Phys. Rev. Lett.* 2007, **98**, 247802.
- 24 S. A. R. Krishnan, W. Weissflog, G. Pelzl, S. Diele, H. Kresse, Z. Vakhovskaya and R. Friedemann, *Phys. Chem. Chem. Phys.*, 2006, **8**, 1170.
- 25 A. Marini and R.Y. Dong, *Phys. Rev. E*, 2011, **83**, 041712.
- 26 S. Kaur, L. Tian, H. Liu, C. Greco, A. Ferrarini, J. Seltmann, M. Lehmann and H. F. Gleeson, *J. Mater. Chem. C*, 2013, **1**, 2416.
- 27 P. Mahboubi Anarjan, N. Noshiranzadeh, R. Bikas, M. Wońska and K. Wozniak, *Acta Crystallogr. E*, 2013, **69**, o102.
- 28 V. M. Chapela, M. J. Percino and C. Rodríguez-Barbarin, *J. Chem. Crystallogr.*, 2003, **33**, 77–83.
- 29 F. H. Allen, *Acta Crystallogr., Sect. B: Struct. Sci.*, 2002, **58**, 380.
- 30 S. H. Hong, R. Verduzco, J. C. Williams, R. J. Twieg, E. DiMasi, R. Pindak, A. Jákli, J. T. Gleeson and S. Sprunt, *Soft Matter*, 2010, **6**, 4819.
- 31 M.J. Frisch, G.W. Trucks, H.B. Schlegel, G.E. Scuseria, M.A. Robb, J.R. Cheeseman, J.A. Montgomery, T. Vreven Jr., K.N. Kudin, J.C. Burant, J.M. Millam, S.S. Iyengar, J. Tomasi, V. Barone, B. Mennucci, M. Cossi, G. Scalmani, N. Rega, G.A. Petersson, H. Nakatsuji, M. Hada, M. Ehara, K. Toyota, R. Fukuda, J. Hasegawa, M. Ishida, T. Nakajima, Y. Honda, O. Kitao, H. Nakai, M. Klene, X. Li, J.E. Knox, H.P. Hratchian, J.B. Cross, C. Adamo, J. Jaramillo, R. Gomperts, R.E. Stratmann, O. Yazyev, A.J. Austin, R. Cammi, C. Pomelli, J.W. Ochterski, P.Y. Ayala, K. Morokuma, G.A. Voth, P. Salvador, J.J. Dannenberg, V.G. Zakrzewski, S. Dapprich, A.D. Daniels, M.C. Strain, O. Farkas, D.K. Malick, A.D. Rabuck, K. Raghavachari, J.B. Foresman, J.V. Ortiz, Q. Cui, A.G. Baboul, S. Clifford, J. Cioslowski, B.B. Stefanov, G. Liu, A. Liashenko, P. Piskorz, I. Komaromi, R.L. Martin, D.J. Fox, T. Keith, M.A. Al-Laham, C.Y. Peng, A. Nanayakkara, M. Challacombe, P.M.W. Gill, B. Johnson, W. Chen, M.W. Wong, C. Gonzalez, J.A. Pople, *Gaussian 03, Revision C.02*, Gaussian, Inc., Wallingford CT, 2004.



**Table of contents entry****Graphical abstract****Textual abstract**

The synthesis and characterization of pyridine bent-core liquid crystals are reported. Some compounds exhibit B1 and B7 mesophase. Lower and wider mesophase ranges are achieved by decreasing polarity of linkers between the pyridine ring and the inner aromatic rings, and increasing length of terminal chains.